TRIBHUVAN UNIVERSITY

INSTITUTE OF ENGINEERING

Pulchowk Campus

Department of Electronics and Computer Engineering

"Brain Image Segmentation using Expectation Maximization and K-Nearest Neighbor Algorithms"

By

BINOD CHANDRA SHRESTHA

(063/MSI/f/603)

A thesis submitted to Department of Electronics and Computer Engineering in partial fulfillment of the requirements for the Degree of Master of Science in Information and Communication Engineering

DEPARTMENT OF ELECTRONICS AND COMPUTER ENGINEERING

LALITPUR, NEPAL

June, 2010

Brain Image Segmentation using Expectation Maximization and K-Nearest Neighbor Algorithms

By

Binod Chandra Shrestha

Roll No: 063/MSI/f/603

Thesis Supervisor:

Prof. Dr. Shashidhar Ram Joshi

Department of Electronics and Computer Engineering

Institute of Engineering

A thesis submitted to Department of Electronics and Computer Engineering in partial fulfillment of the requirements for the Degree of Master of Science in Information and Communication Engineering

Department of Electronics and Computer Engineering

Institute of Engineering, Pulchowk Campus

Tribhuvan University

Llitpur, Nepal

June, 2010

This thesis is dedicated to

My Parents

Late Narayan Kumar Shrestha

&

Mrs. Laxmi Shrestha

Certificate of Recommendation

The undersigned certify that we have read the thesis report and recommended to the Institute of Engineering for acceptance, this thesis report entitled "**Brain Image Segmentation using Expectation Maximization and K-Nearest Neighbor Algorithms"** submitted by **Mr. Binod Chandra Shrestha** in partial fulfillment of the requirement for the award of the degree of **"Master of Science in Information and Communication Engineering".**

Supervisor:

Prof. Dr. Shashidhar Ram Joshi
Department of Electronics and Computer Engineering
Institute of Engineering
Tribhuvan University
Pulchowk, Nepal

MSICE Program Coordinator:

Asst. Prof. Sharad Ghimire
Department of Electronics and Computer Engineering
Institute of Engineering
Tribhuvan University
Pulchowk, Nepal

External Examiner:

Departmental Acceptance

This thesis entitled "**Brain Image Segmentation using Expectation Maximization and K-Nearest Neighbor Algorithms"** submitted by **Mr. Binod Chandra Shrestha** in partial fulfillment of the requirement for the award of the degree of **"Master of Science in Information and Communication Engineering"** has been accepted as a bonafide record of work independently carried out by him in the department.

Prof. Dr. Shashidhar Ram Joshi

Department of Electronics and Computer Engineering

Institute of Engineering

Tribhuvan University

Pulchowk, Nepal

ACKNOWLEDGEMENT

I would like to express my sincere gratitude to my supervisor Prof. Dr. Shashidhar Ram Joshi for valuable suggestion and guideline throughout the thesis. I would like to express gratefulness to Asst. Prof. Sharad Kumar Ghimire, Program Coordinator, Master of Science in Information and Communication Engineering, IOE, Pulchowk Campus for providing me the necessary suggestion throughout this thesis. I would like to heartily thank to my wife Mrs. Akshata Shrestha for her patience and providing me inspiring environment. I want acknowledge to all the staffs of Department of Electronics and Computer Engineering, IOE, Pulchowk Campus, Library IOE, Pulchowk Campus and Advanced College of Engineering and Management and Smart House of Technology and Research P. Ltd. for their kind support.

Finally, I would like to thank all the persons who directly or indirectly help me throughout this thesis work.

Binod Chandra Shrestha
063/msi-f/603

ABSTRACT

Segmentation of an image entails the division or separation of the image into regions of similar attribute. Segmentation is one of the main problems in image analysis. Expectation Maximization (EM) and K-Nearest Neighbor (KNN) Algorithms have been used for segmentation of Magnetic Resonance (MR) image of brain.

The main objective of this thesis is to segment and classify brain image into Gray Matter (GM), White Matter (WM) and Cerebral Spinal Fluid (CSF) using EM algorithm and KNN algorithm.

TABLE OF CONTENTS

LIST OF TABLES

LIST OF FIGURES

LIST OF ABBREVIATIONS

CAT	Computer Axial Tomography
CSF	Cerebral Spinal Fluid
EM	Expectation Maximization
GM	Gray Matter
k-NN	k Nearest Neighbor
LoG	Laplacian of Gaussian
ML	Maximum Likelihood
MRI	Magnetic Resonance Imaging
PD	Proton Density
WM	White Matter

CHAPTER 1

Introduction

1.1. Background

Medical image processing can be thought of as a specialization of signal processing techniques and their application to the two-dimensional (2D) domain, in the case of still images, or three dimensional (3D) domains for volumetric images or video sequences. A wide number of issues exist here such as image acquisition and coding, image reconstruction, image enhancement and denoising, and image analysis.

The segmentation [1] is an image analysis technique. The term segmentation is usually used to describe the process of selecting a specific object or objects from an image. There are three approaches to segmentation of images: manual segmentation, automatic segmentation and semiautomatic segmentation. Manual segmentation involves an expert observer outlining the object of interest in the image on computer screen or paper or film. Manual segmentation is very time consuming, subject to human error and has poor intra-observer reproducibility. In automatic segmentation, image processing tools are used. There should be proper match between references set of images and test images. Semiautomatic segmentation is compromise between the two approaches. The human observer usually starts the segmentation, and has opportunity to make corrections, but as of work as possible is automated. In this thesis, semiautomatic segmentation approach is used.

On a higher level, automatic or user-assisted techniques [2] may be used to segment and detect specific objects in an image, e.g., organs in a computed axial tomography (CAT) slice or process and visualize volumetric data. Progress in medical imaging coincides not only with the advent of maturing processing techniques, but also with the introduction of better acquisition equipment and the integration of knowledge-based strategies. Regarding complexity and tackling of novel concepts, the arrival of magnetic resonance imaging (MRI) and other related acquisition techniques that produce 3D or higher resolution images paved the way for visualization applications and model-driven approaches. In the field of 2D imaging image registration, segmentation, and pattern recognition and classification [2] are still in the forefront of interest. In the case of segmentation, knowledge-based approaches that are constantly integrated even into specialized equipment provide for tackling problems such as edge detection and region growing, and subsequent object boundary detection. CAT and MRI scans are eminent examples of such techniques, since lower level segmentation of image intensity can be combined with knowledge of tissue structure and positioning to cater for organ detection and segmentation.

There are Different approaches to gray and white matter measurements in magnetic resonance imaging (MRI) [3] and [4]. For clinical use, the estimated values must be reliable and accurate when, unfortunately, many techniques fail on these criteria in an unrestricted clinical environment. A recent method for tissue clusterization [3] in MRI analysis has the advantage of great simplicity, and it takes the account of partial volume effects. Intensity group clustering algorithms are proposed to achieve further diagnosis for brain MRI. This technique makes use of image tissue biases of intensity value pixels to provide 2 regions of interest as techniques. Moreover, the original mathematic solution could still be used with a specific set of modern sequences. There are many advantages to generalize the solution, which give far more scope for application and greater accuracy.

1.2. Problem Statement

Image segmentation has received extensive attention since the early years of computer vision research. The segmentation remains one of the main problems in image analysis. In medical diagnosis, there should be proper segmentation and classification of abnormal tissues from normal tissues. A doctor can segment the brain image manually using his/ her expertise but it takes a long time.

Image segmentation is the first step in image analysis. Brain tissue is particularly complex structure and its segmentation is an important task for many purposes including diagnostic and therapeutic uses for delineation of abnormal areas to be treated prior to radio surgery, delineation of abnormal tissues before and after surgery. The segmentation MR image of brain into CSF, Gray Matter and White Matter is the main field of interest.

1.3. Objective

The thesis is focused on segmentation of medical images using different algorithms of image processing. In general, this thesis has following objective:

1. To segment CSF, Gray Matter and White Matter presented on MR image of brain using EM and k-NN algorithms.

1.4. Organization of Thesis

This chapter describes background, problem statement and objective of this thesis. The remainder of this thesis is organized as follows:

Chapter 2 deals with literature review with overview of image segmentation and components of brain image.

Chapter 3 describes methodology for segmentation of images that implemented on this thesis.

Chapter 4 describes about simulation environment including materials used, software and hardware used in this thesis.

Chapter 5 explains implementation of the expectation maximization and k nearest neighbor algorithms for segmentation of MR images of brain.

Finally, chapter 6 concludes the thesis and describes about the future enhancement.

CHAPTER 2

Literature Review

2.1. Overview of Image Segmentation

Medical image segmentation is an essential step for most subsequent image analysis tasks. The segmentation of anatomic structure [3] in the brain plays a crucial role in Nero imaging analysis. Successful numerical algorithms can help researchers, physicians and neurosurgeons to investigate and diagnose the structure and function of the brain in both health and disease [5]. This has motivated the need for segmentation techniques that are robust in application involving a broad range of anatomic structure, disease and image type. The problems associated with segmentation have been well studied and a large number of approaches have been developed, many specific to a particular image. General approaches to segmentation can be grouped into three classes: pixel-based methods, regional methods, and edge based methods [6] and [7].

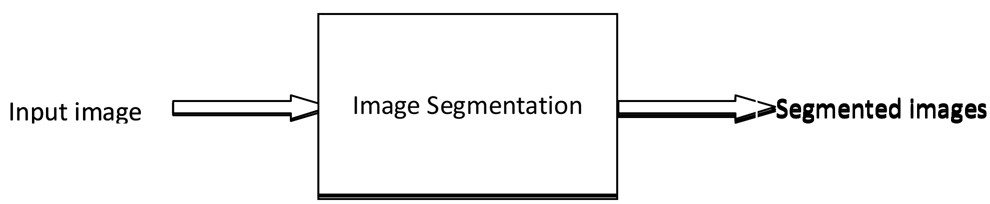

Figure 2.1 Block diagram of image segmentation

2.1.1 Pixel Based Method

The most straightforward and common of the pixel-based methods is thresholding [1] in which all pixels having intensity values above, or below, some level are classified as part of the segment. Thresholding is usually quite fast and can be done in real time allowing for interactive setting of the threshold. The basic concept of thresholding can be extended to include both upper and lower boundaries, an operation termed slicing since it isolates a specific range of pixels. Slicing can be generalized to include a number of different upper and lower boundaries, each encoded into a different number. A major concern in these pixel-based methods is setting the threshold or slicing level(s) appropriately. Usually these levels are set by the program, although in some situations they can be set interactively by the user. Finding an appropriate threshold level can be aided by a plot of pixel intensity distribution over the whole image, regardless of whether you adjust the pixel level interactively or automatically. Such a plot is termed the intensity histogram plot. Another histogram-based strategy that can be used if the distribution is bimodal is to assume that each mode is the result of a unimodal, Gaussian distribution [2]. An estimate is then made of the underlying distributions, and the point at which the two estimated distributions intersect should provide the optimal threshold. The principal problem with this approach is that the distributions are unlikely to be truly Gaussian.

2.1.2 Regional Based Method

These approaches look for similarities or consistency in the search for structural units. These approaches can be very effective in segmentation tasks, but they all suffer from a lack of edge definition. This is because they are based on neighborhood operations and these tend to blur edge regions, as edge pixels are combined with structural segment pixels. The larger the neighborhood used, the more poorly edges will be defined. Unfortunately, increasing neighborhood size usually improves the power of any given continuity-based operation, setting up a compromise between identification ability and edge definition. One easy technique that is based on continuity is low pass filtering. Since a low pass filter is a sliding neighborhood operation that takes a weighted average over a region, it enhances consistent characteristics.

Morphological operations have to do with processing shapes. In this sense they are continuity-based techniques, but in some applications they also operate on edges, taking them useful in edge-based approaches as well. In fact, morphological operations have many image processing applications in addition to segmentation. The two most common morphological operations are dilation and erosion. In dilation the rich get richer and in erosion the poor get poorer. Specifically, in dilation, the center or active pixel is set to the maximum of its neighbors, and in erosion it is set to the minimum of its neighbors. Since these operations are often performed on binary images, dilation tends to expand edges, borders, or regions, while erosion tends to decrease or even eliminate small regions. Obviously, the size and shape of the neighborhood used will have a very strong influence on the effect produced by either operation [6] and [7].

2.1.3 Edge Based Method

Edge-based methods were the first set of tools developed for segmentation. To move from edges to segments, it is necessary to group edges into chains that correspond to the sides of structural units, i.e., the structural boundaries. Approaches vary in how much prior information they use, that is, how much is used of what is known about the possible shape. False edges and missed edges are two of the more obvious, and more common, problems associated with this approach. The first step in edge-based methods is to identify edges which then become candidates for boundaries.

In this method the image is segmented on the basis of its profile. Thus, contour following, connectivity, edge linking and graph searching, curve fitting, Hough Transform etc are applicable to image segmentation [6] and [7].

2.2 Introduction to MRI

The main contents of human body are fat and water. The fat and water contains around 63% of hydrogen atoms [8]. Nucleus of hydrogen atom has high affinity with magnetic field. So, Magnetic Resonance Imaging (MRI) uses Nuclear Magnetic Resonance from the hydrogen nuclei.

MRI is the most frequently used non invasive imaging technique in clinical neuroscience and neuro-surgery for non-invasively establishing diagnosis. Because of the absence of ionizing radiation, as opposed to other imaging methods such as X-ray and CT produces images in planes with any orientation and superior contrast resolution of soft tissue, such as pathologic tissues e.g. tumor, MRI has become popular. Nowadays MRI has become an essential tool for the diagnosis of central nervous system. MRI can identify different soft tissue structures e.g. blood, blood vessels, fluids etc. But bone and bone like structures are studied by other imaging techniques e.g. X-ray and CT.

The resonance is the exchange of energy between two systems at a specific frequency. MRI is based on proton density and proton relaxation dynamics. The energetic interaction between the electromagnetic radio frequency and protons spin with the same frequency the frequency is called Lamor frequency. The protons subsequently release the absorbed energy and relax back to the original alignment at a rate determined by the T_1 and T_2 relaxation times. The return of the nuclei to their initial to their initial state is governed by two physical process:

- T_1: longitudinal relaxation corresponds to longitudinal magnetization recovery.
- T_2: transverse relaxation corresponds to transverse magnetization decay.

The strength of the MRI signal depends on three parameters: T1, T2 and proton density (PD) in a tissue, the greater the PD, the larger the signal will be.

Pulse Sequence	Effect	Tissues
PD	High Proton density (bright) Low proton density (dark)	Fluids and fat Calcium, cortical bone, fibrous tissue, air
T_1	Short T_1 relaxation (bright) Long T_1 relaxation (dark)	Fat, liquid containing molecules, protein Neoplasm, edema, CSF, pure fluid, Inflammation
T_2	Short T_2 relaxation (dark) Long T_2 relaxation (bright)	Iron containing substance Neoplasm, Edema, CSF, pure fluid, Inflammation

Table 2.1 Effect of pulse sequences for different tissue types [8]

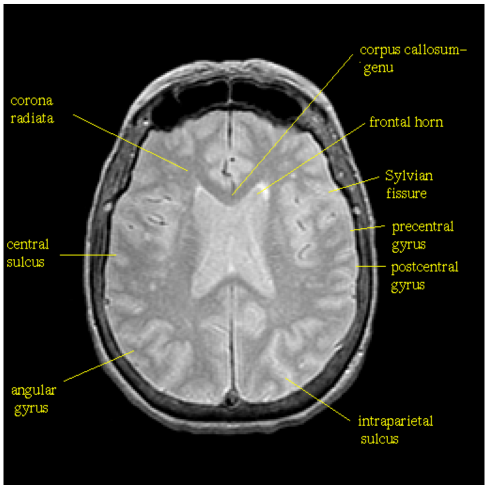

(a)

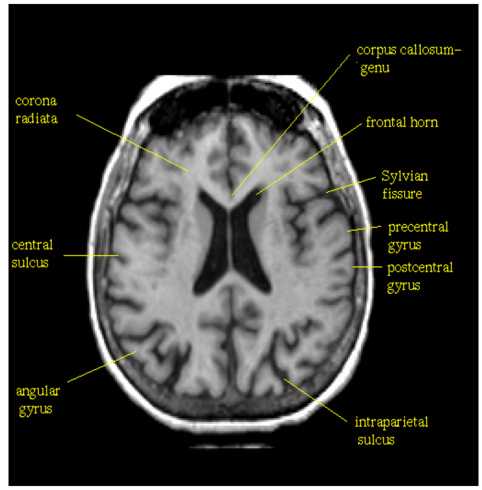

(b)

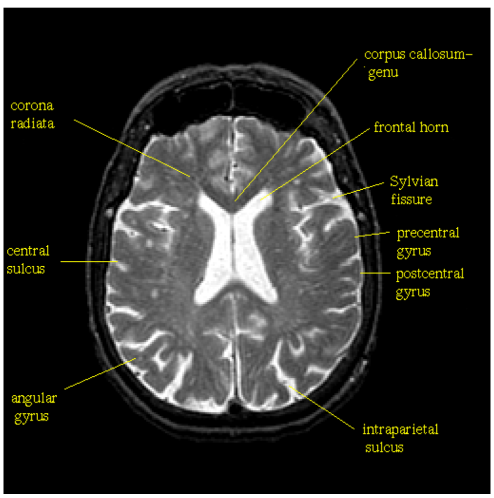

(c)

Figure 2.2 MR image (a) PD weighted, (b) T_1 weighted and (c) T_2 weighted [8]

2.3 Components of Brain

There are three major components of brain. They are gray matter (GM), white matter (WM) and cerebral spinal fluid (CSF) [4] and [8].

2.3.1 Gray Matter

Gray matter is one of the major components of central nervous system. It consists neuronal cell bodies, neuropil (dendrite and both unmyelinated axons and myelinated axons), glial cells (astroglia and oligodendrocytes) and capillaries. Gray matter is distributed at the surface of cerebral hemisphere and cerebellum, as well as the depth of the cerebrum, cerebellar, brainstem and spinal gray matter. The function of gray matter is to route sensory or motor stimulus to inter-neurons of central nervous system in order to create a response to the stimulus through chemical synapse activity.

2.3.2 White Matter

White matter is one of major components of central nervous system. It consists mostly of myelinated axons. White matter is composed of bundle of mylinated nerve cell processes, which connect various gray matter areas of the brain to each other, and carry impulse between neurons. The white matter is the tissue through which messages between different areas of gray matter within the nervous system.

2.3.3 Cerebral Spinal Fluid

Cerebrospinal fluid is a clear bodily fluid that occupies the subarachnoid space and the ventricular system around and inside the brain. It constitutes the content of all itra-cerebral ventricles, cisterns, and sulci, as well as the central canal of the spinal cord. It acts as buffer for the cortex, providing a basic mechanical and immunological protection to the brain inside the skull.

CHAPTER 3

Methodology

3.1. Expectation Maximization (EM)

Expectation maximization (EM) [1], [3], [9] and [10] is optimization method for evaluation of maximum likelihood (ML) [11] estimates. EM algorithm relies on the concept of complete data space to be selected in some conventional way.

3.1.1. The Density Estimation

The density estimation [1] problem can be defined as follows: given a set of N points in D dimensions, $x_1,\dots\dots\dots,x_N \in R^D$, and a family F of probability density functions on R^D, find the probability density f(x) $\in$ F that is most likely to have generated the given points. One way to define the family F is to give each of its members the same mathematical form, and to distinguish different members by different values of a set of parameters θ. For example, the functions in F could be mixtures of Gaussian functions.

$$f(x;\theta) = \sum_{k=1}^{K} p_k \; g(x;\mu_k,\sigma_k) \dots\dots\dots\dots\dots\dots\dots\dots\dots\dots\dots\dots\dots\dots\dots\dots\dots\dots\dots\dots \quad (1)$$

Where,

$$p_k \geq 0 \;\&\; \sum p_k = 1 \dots\dots\dots\dots\dots\dots\dots\dots\dots\dots\dots\dots\dots\dots\dots\dots\dots\dots\dots\dots\dots\dots\dots\dots .. \quad (2)$$

and

$$g(x;\mu_k,\sigma_k) = \frac{1}{\sqrt{2\pi\sigma^2}}\exp(-\frac{(x-\mu)^2}{2\sigma^2}) \dots\dots\dots\dots\dots\dots\dots\dots\dots\dots\dots\dots\dots\dots ... \quad (3)$$

is Gaussian distribution is a continuous probability distribution that often gives a good description of data that cluster around the mean. The continuous probability density function of the Gaussian distribution exists only when the parameter variance σ^2 is not zero. The numbers p_k are called mixing probabilities.

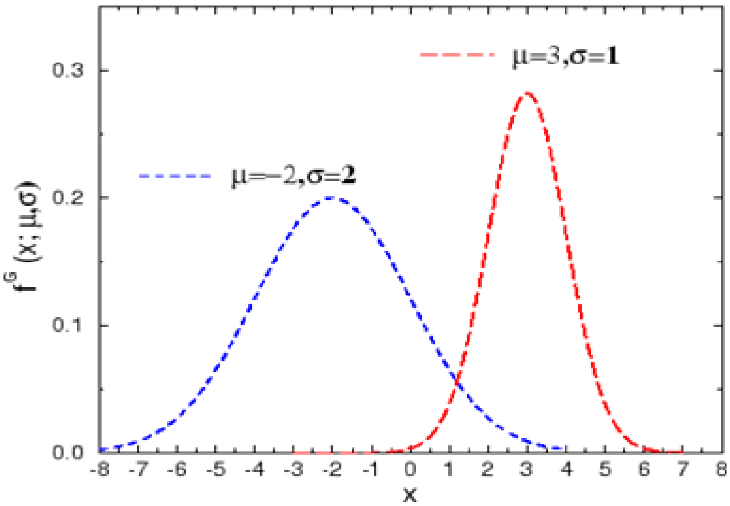

Figure 3.1 Gaussian distribution

Mixtures of Gaussian functions are obviously well-suited to modelling clusters [2] of points: each cluster is assigned a Gaussian, with its mean somewhere in the middle of the cluster, and with a standard deviation that somehow measures the spread of that cluster.

- Draw a random integer between 1 and K with probability p_k of drawing k. This selects the cluster from which to draw point x_n.
- Draw a random D-dimensional real vector $x_n \in R^D$ from the k-th Gaussian density $g(x; m_k, \sigma_k)$.

This is called a generative model for the given set of points.

Since the family of mixtures of Gaussian functions is parametric, the density estimation problem can be defined more specifically as the problem of finding the vector θ of parameters that specifies the model from which the points are most likely to be drawn.

What remains to be determined is the meaning of “most likely.” Let a function $\Lambda(X; \theta)$ that measures the likelihood of a particular model given the set of points: the set X is fixed, because the points x_n are given, and Λ is required to be large for those vectors θ of parameters such that the mixture of Gaussian functions $f(x; \theta)$ is likely to generate sets of points like the given one.

Bayesians will derive Λ from Bayes's theorem, but at the cost of having to specify a prior distribution for θ itself. The more straightforward Maximum Likelihood approach is taken: the probability of drawing a value in a small volume of size dx around x is f(x; θ) dx. If the random draws in the generative model are independent of each other, the probability of drawing a sample of N points where each point is in a volume of size dx around one of the given x_n is the product $f(x_1; \theta)$ dx … $f(x_N; \theta)$ dx. Since the volume dx is constant, it can be ignored when looking for the θ that yields the highest probability, and the likelihood function can be defined as follows:

$$\Lambda(X;\theta) = \prod_{n=1}^{N} f(x_n;\theta) \dots\dots (4)$$

For mixture of Gaussian functions, we have:

$$\Lambda(X;\theta) = \prod_{n=1}^{N}\sum_{k=1}^{K} p_k\ g(x_n;\mu_k,\sigma_k) \dots\dots (5)$$

the parametric density estimation problem can be defined more precisely as follows:

$$\theta = \arg\max_{\theta} \Lambda(X;\theta) \dots\dots (6)$$

3.1.2. Histogram

Histogram [12] is a graphical display of tabular frequencies. An image histogram is a type of histogram which acts as a graphical representation of the tonal distribution in a digital image. The histogram of a digital image with gray levels in the range [0, L-1] is a discrete function:

$$h(r_k) = n_k \dots\dots (7)$$

Where r_k is k^{th} gray level and n_k is the number of pixels in the image having gray level r_k.

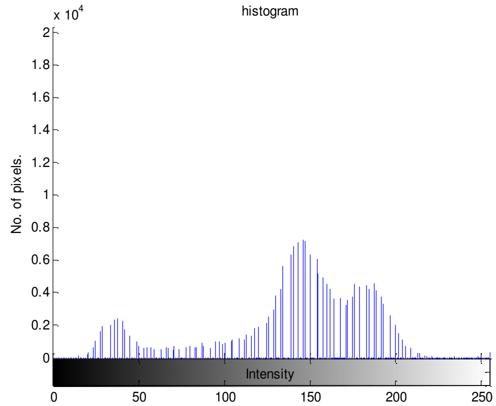

Figure 3.2 Histogram of an image

3.1.3. Thresholding

Thresholding is the process of binarization [1] of an image. It is the simplest method of image segmentation. During the thresholding process, individual pixels in an image are marked as "object" pixels if their value is greater than some threshold value (assuming an object to be brighter than the background) and as "background" pixels otherwise.

3.1.4. EM Algorithm

Expectation maximization is one of the most common algorithms used for density estimation of data points in an unsupervised setting. The algorithm relies on finding the maximum likelihood estimates of parameters when the data model depends on certain latent variables. In EM algorithm, alternating steps of expectation (E) and maximization (M) are performed iteratively till the results converge [3].

Suppose approximate estimates $p_k^{(i)}$, $\mu_k^{(i)}$, $\sigma_k^{(i)}$ are avaiable for the parameters of the likelihood function $\Lambda(X;\ \theta)$ or its logarithm $\lambda(X;\ \theta)$. Now, better estimates $p_k^{(i+1)}$, $\mu_k^{(i+1)}$, $\sigma_k^{(i+1)}$ can be computed by first using old estimate to construct a lower bound $b_i(\theta)$ for the likelihood function, and then maximizing the bound with respect to p_k, m_k, σ_k. The EM starts with initial values $p_k^{(0)}$, $\mu_k^{(0)}$, $\sigma_k^{(0)}$ for the parameters and iteratively performs these two steps until convergence. Construction of the bound $b_i(\theta)$ is called the E- step and maximization of $b_i(\theta)$ that gives the new estimates $p_k^{(i+1)}$, $\mu_k^{(i+1)}$, $\sigma_k^{(i+1)}$ is called the M-step.

If the old parameter estimates $p_k^{(i)}$, $\mu_k^{(i)}$, $\sigma_k^{(i)}$, we can compute $p^i(k|n)$ in E-step:

$$p^i(k|n) = \frac{p_k^{(i)}\ g(x_n; \mu_k, \sigma_k)}{\sum_{m=1}^{K} p_k^{(i)}\ g(x_n; \mu_k, \sigma_k)} \ldots\ldots\ldots\ldots\ldots\ldots\ldots\ldots\ldots\ldots\ldots\ldots\ldots. (8)$$

The log maximum likelihood function is given by:

$$\begin{aligned}\lambda(\mathrm{X};\ \theta) &= \sum_{n=1}^{N} \log \sum_{k=1}^{K} p_k\ g(x_n; \mu_k, \sigma_k) \\ &\geq \sum_{n=1}^{N} \sum_{k=1}^{K} p^i(k|n) \log\left(\frac{p_k\ g(x_n; \mu_k, \sigma_k)}{p^i(k|n)}\right) \\ &= b_i\ (\theta) \ldots\ldots\ldots\ldots\ldots\ldots\ldots\ldots\ldots\ldots\ldots\ldots\ldots\ldots\ldots\ldots\ldots\ldots\ldots\ldots\ldots.. (9)\end{aligned}$$

The derivative of $b_i(\theta)$ with respect to μ_k is easily found as:

$$\frac{\partial(\theta)}{\partial \mu_k} = \sum_{n=1}^{N} p^i(k|n) \frac{\mu_k - x_n}{\sigma_k^2} \ldots\ldots\ldots\ldots\ldots\ldots\ldots\ldots\ldots\ldots\ldots\ldots\ldots.. (10)$$

Setting equation (10) to zero we get,

$$\mu_k \sum_{n=1}^{N} p^i(k|n) = \sum_{n=1}^{N} p^i(k|n)\ x_n \ldots\ldots\ldots\ldots\ldots\ldots\ldots\ldots\ldots\ldots\ldots\ldots (11)$$

Solving iteratively we get

$$\mu_k^{(i+1)} = \frac{\sum_{n=1}^{N} p^i(k|n)\ x_n}{\sum_{n=1}^{N} p^i(k|n)} \ldots\ldots\ldots\ldots\ldots\ldots\ldots\ldots\ldots\ldots\ldots\ldots\ldots\ldots\ldots.. (12)$$

And equestion (9) yields

$$\sigma_k^{(i+1)} = \sqrt{\frac{\sum_{n=1}^{N} p^i(k|n) \left\| x_n - \mu_k^{(i+1)} \right\|^2}{D \sum_{n=1}^{N} p^i(k|n)}} \ldots\ldots\ldots\ldots\ldots\ldots\ldots\ldots\ldots (13)$$

The new estimate for mixing probabilities as a function of the old membership probabilities:

$$p_k^{(i+1)} = \frac{1}{N}\sum_{n=1}^{N} p^i(k|n) \ldots\ldots\ldots\ldots\ldots\ldots\ldots\ldots\ldots\ldots\ldots\ldots\ldots\ldots\ldots\ldots\ldots\ldots\ldots (14)$$

In M-step, parameters $p_k^{(i+1)}$, $\mu_k^{(i+1)}$, $\sigma_k^{(i+1)}$ are computed.

3.2. k- Nearest Neighbor (k-NN)

*k- n*earest neighbor or k-NN classification [13] determines the decision boundary locally. For 1NN each document is assigned to the class of its closest neighbor. For kNN assign each document is assigned to the majority class of its k closest neighbors where k is a parameter. The rationale of kNN classification is that, based on the contiguity hypothesis, a test data d is expected to have the same label as the training data located in the local region surrounding d.

3.2.1. k- NN Algorithm

The k nearest neighbor (k-NN) is a popular supervised classification algorithm with asymptotic optimum properties. It is nonparametric supervised pattern classification technique [13]. It works based on minimum distance from the query instance to the training samples to determine the k-nearest neighbors. After gathering k nearest neighbors, simple majority of k-nearest neighbors are taken to the prediction of query instance. Usually Euclidean distance is used as the distance metric; however this is only applicable to continuous variables. In cases such as text classification, another metric such as the Hamming distance can be used.

The data for k-NN algorithm consist of several multivariate attributes name X_i that will be used to classify Y. the data of k-NN can be any measurement scale from ordinal, nominal, to quantitative scale but for the moment let us deal with only quantitative X_i and nominal Y.

The algorithm is explained below.

1. Determine the parameter k = number of nearest neighbors X_i beforehand. This value is all up to us.
2. Calculate the distance between the query-instance and all the training samples. Any distance algorithm can be used. Generally Euclidean distance is taken. Say, the query instance have coordinates (x_1^q, x_2^q) and the coordinate of training sample is (x_1^t, x_2^t) then,

$$d^2 = (x_1^t - x_1^q)^2 + (x_2^t - x_2^q)^2 \ldots\ldots\ldots\ldots\ldots\ldots\ldots\ldots\ldots\ldots\ldots\ldots\ldots (15)$$

3. Sort the distances for all the training samples and determine the nearest neighbor based on the k-th minimum distance.
4. Since this is supervised learning, get all the Categories of our training data for the sorted value which fall under k.
5. Use the majority of nearest neighbors as the prediction value.

3.2.2. Parameter Selection

The best choice of k depends upon the data; usually, larger values of k reduce the effect of noise on the classification, but make boundaries between classes less distinct. A good k can be selected by various heuristic techniques, for example, cross-validation. The special case where the class is predicted to be the class of the closest training sample is called the nearest neighbor algorithm.

The accuracy of the k-NN algorithm can be severely degraded by the presence of noisy or irrelevant features, or if the feature scales are not consistent with their importance. Much research effort has been put into selecting or scaling features to improve classification. A particularly popular approach is the use of evolutionary algorithms to optimize feature scaling. Another popular approach is to scale features by the mutual information [14] of the training data with the training classes.

3.3. Edge Detection

Edge detection [7] is a problem of fundamental importance in image analysis. Edges characterize object boundaries and are therefore useful for segmentation, registration, and identification of objects in a scene. The goal of edge detection is the detection and characterization of significant intensity changes i.e. the detection of meaningful discontinuities in gray level. Edge based segmentation represents a large group of methods based on information based on information about edges in the images. These methods rely on the edges found in an image by edge detecting operators which mark the edges in the image location of discontinuities in gray level, color, texture etc.

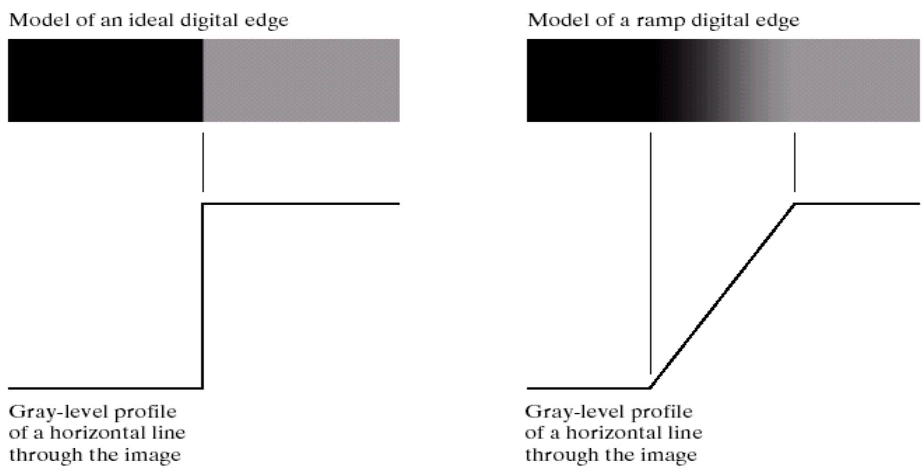

Figure 3.3 Model of edges [7]

An edge is set on connected pixels that lie on the boundary between two regions. A regional definition of edge requires the abilities to measure gray level transitions in a meaningful way. An ideal edge is a set of connected pixels, each of which is located at an orthogonal step transition in gray level. The image affected by the acquisition imperfections yields the blurred image resulting the edges with ramp like profile. The slope of ramp is proportional to the degree of blurring in the edge and thickness of the edge is determined by the length of ramp resulting blurred texture to have thick edge and sharp texture to have thin edge.

The biggest drawback to edge detection methods of image segmentation is the sensitivity to the size and type of smoothing and derivative convolution masks applied to the original image. In some cases these two masks are not parameterized and therefore not under the user control. This limits the applicability of these algorithms to different types of images. Most edge detection algorithms are very sensitive to noise and can yield edge information that is not a boundary between regions in an image. Furthermore, edges that are computed are often not linked where contiguity exists in the image edge linking algorithm can be used for this purpose. Edge detection techniques like the Sobel [6], Prewitt [7] operators are based on convolution in very small neighborhoods and work well for specific images only. The main disadvantage of these edge detectors is their dependence on the size of objects and sensitivity to noise. An edge detection technique based on zero crossings [7] of second order derivative explores the fact that a step edge corresponds to an abrupt change in the image image function. The first derivative of the image function should have an extreme value at the position corresponding to edge in the image, and so the second derivative should be zero at the same position.

The texture of MR image is composed of complex tissues structure with gaussian distributed intensity levels and edge badge based segmentation techniques are inappropriate approach for the segmentation of MR images. Gaussian smoothing of the image prior to the application of the Laplacian detector can help to some extent to find out the robust edge. In this section, Laplacian, Sobel, Prewitt, Canny Edge, and Laplacian of Gaussian detector are described [6] and [7].

3.3.1. Sobel Operator

The operator consists of a pair of 3×3 convolution kernels as shown in Figure 1. One kernel is simply the other rotated by 90°.

-1	0	+1
-2	0	+2
-1	0	+1

G_x

+1	+2	+1
0	0	0
-1	-2	-1

G_y

Figure 3.4 Masks used by Sobel Operator [7]

These kernels are designed to respond maximally to edges running vertically and horizontally relative to the pixel grid, one kernel for each of the two perpendicular orientations. The kernels can be applied separately to the input image, to produce separate measurements of the gradient component in each orientation (call these G_x and G_y). These can then be combined together to find the absolute magnitude of the gradient at each point and the orientation of that gradient. The gradient magnitude is given by:

$$|G| = \sqrt{G_x^2 + G_y^2} \quad \ldots\ldots\ldots\ldots\ldots\ldots\ldots\ldots\ldots\ldots (16)$$

Typically, an approximate magnitude is computed using:

$$|G| = |G_x| + |G_y| \quad \ldots\ldots\ldots\ldots\ldots\ldots\ldots\ldots\ldots\ldots (17)$$

which is much faster to compute.

The angle of orientation of the edge (relative to the pixel grid) giving rise to the spatial gradient is given by:

$$\theta = \tan^{-1}\left(\frac{G_y}{G_x}\right) \quad \ldots\ldots\ldots\ldots\ldots\ldots\ldots\ldots\ldots\ldots (18)$$

3.3.2. **Robert's cross operator**:

The Roberts Cross operator [7] performs a simple, quick to compute, 2-D spatial gradient measurement on an image. Pixel values at each point in the output represent the estimated absolute magnitude of the spatial gradient of the input image at that point. The operator consists of a pair of 2×2 convolution kernels as shown in Figure 2. One kernel is simply the other rotated by 90°. This is very similar to the Sobel operator.

+1	0
0	-1

Gx

0	+1
-1	0

Gy

Figure 3.5 Masks used for Robert operator [7]

These kernels are designed to respond maximally to edges running at 45° to the pixel grid, one kernel for each of the two perpendicular orientations. The kernels can be applied separately to the input image, to produce separate measurements of the gradient component in each orientation (call these G_x and G_y). These can then be combined together to find the absolute magnitude of the gradient at each point and the orientation of that gradient. The gradient magnitude is given by:

$$|G| = \sqrt{G_x^2 + G_y^2} \dots\dots\dots\dots\dots\dots\dots\dots\dots\dots\dots\dots\dots\dots\dots\dots\dots\dots\dots\dots (19)$$

although typically, an approximate magnitude is computed using:

$$|G| = |G_x| + |G_y| \dots\dots\dots\dots\dots\dots\dots\dots\dots\dots\dots\dots\dots\dots\dots\dots\dots\dots\dots .. (20)$$

which is much faster to compute.

The angle of orientation of the edge giving rise to the spatial gradient (relative to the pixel grid orientation) is given by:

$$\theta = \tan^{-1}(\frac{G_y}{G_x}) - \frac{3\pi}{4} \dots\dots\dots\dots\dots\dots\dots\dots\dots\dots\dots\dots\dots\dots\dots\dots\dots\dots\dots\dots (21)$$

3.3.3. Prewitt's operator:

Prewitt operator is similar to the Sobel operator and is used for detecting vertical and horizontal edges in images.

+1	+1	+1
0	0	0
-1	-1	-1

G_x

-1	0	+1
-1	0	+1
-1	0	+1

G_y

Figure 3.6 Masks for the Prewitt gradient edge detector [7]

3.3.4. Laplacian of Gaussian:

The Laplacian [7] is a 2-D isotropic measure of the 2nd spatial derivative of an image. The Laplacian of an image highlights regions of rapid intensity change and is therefore often used for edge detection. The Laplacian is often applied to an image that has first been smoothed with something approximating a Gaussian Smoothing filter in order to reduce its sensitivity to noise. The operator normally takes a single gray level image as input and produces another gray level image as output.

The Laplacian *L(x,y)* of an image with pixel intensity values *I(x,y)* is given by:

$$L(x, y) = \frac{\partial^2 I}{\partial x^2} + \frac{\partial^2 I}{\partial y^2} \dots\dots\dots\dots\dots\dots\dots\dots\dots\dots\dots\dots\dots\dots\dots\dots\dots\dots\dots\dots (22)$$

Since the input image is represented as a set of discrete pixels, a discrete convolution kernel has to find that can approximate the second derivatives in the definition of the Laplacian. Three commonly used small kernels are shown in Figure 3.7.

0	1	0
1	-4	1
0	1	0

1	1	1
1	-8	1
1	1	1

-1	2	-1
2	-4	2
-1	2	-1

Figure 3.7 Three commonly used discrete approximations to the Laplacian filter [7]

Because these kernels are approximating a second derivative measurement on the image, they are very sensitive to noise. To counter this, the image is often Gaussian Smoothed before applying the Laplacian filter. This pre-processing step reduces the high frequency noise components prior to the differentiation step.

In fact, since the convolution operation is associative, the Gaussian smoothing filter can convolved with the Laplacian filter first of all, and then convolve this hybrid filter with the image to achieve the required result. Doing things this way has two advantages: Since both the Gaussian and the Laplacian kernels are usually much smaller than the image, this method usually requires far fewer arithmetic operations.

The LoG (`Laplacian of Gaussian') kernel can be pre-calculated in advance so only one convolution needs to be performed at run-time on the image.

The 2-D LoG function centered on zero and with Gaussian standard deviation σ has the form:

$$LoG(x,y) = \frac{1}{\pi\sigma^4}\left(1 - \frac{(x^2 + y^2)}{2\sigma^2}\right)\exp\left(-\frac{x^2 - y^2}{2\sigma^2}\right) \ldots\ldots\ldots\ldots\ldots\ldots\ldots\ldots\ldots\ldots\ldots. (23)$$

and is shown in Figure 3.8.

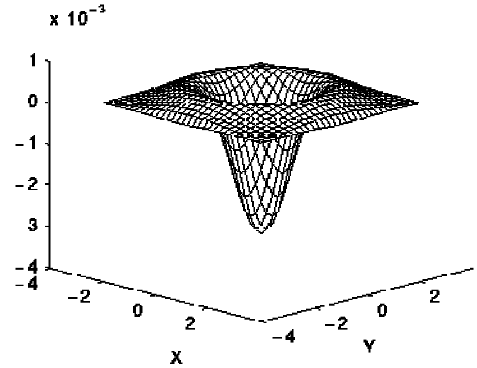

Figure 3.8 The 2-D LoG function. The *x* and *y* axes are marked in standard deviations (σ).

A discrete kernel that approximates this function (for a Gaussian σ = 1.4) is shown in Figure 3.9.

0	1	1	2	2	2	1	1	0
1	2	4	5	5	5	4	2	1
1	4	5	3	0	3	5	4	1
2	5	3	-12	-24	-12	3	5	2
2	5	0	-24	-40	-24	0	5	2
2	5	3	-12	-24	-12	3	5	2
1	4	5	3	0	3	5	4	1
1	2	4	5	5	5	4	2	1
0	1	1	2	2	2	1	1	0

Figure3.9 Discrete approximation to LoG function with Gaussian σ = 1.4 [7]

3.3.5. Canny Edge Detection

The Canny edge detection algorithm [6] and [7] is known to many as the optimal edge detector. Canny's intentions were to enhance the many edge detectors already out at the time he started his work. The first and most obvious is low error rate. It is important that edges occurring in images should not be missed and that there be no responses to non-edges. The second criterion is that the edge points be well localized. In other words, the distance between the edge pixels as found by the detector and the actual edge is to be at a minimum. A third criterion is to have only one response to a single edge. This was implemented because the first two were not substantial enough to completely eliminate the possibility of multiple responses to an edge.

Based on these criteria, the canny edge detector first smoothes the image to eliminate and noise. It then finds the image gradient to highlight regions with high spatial derivatives. The algorithm then tracks along these regions and suppresses any pixel that is not at the maximum. The gradient array is now further reduced by hysteresis. Hysteresis is used to track along the remaining pixels that have not been suppressed. Hysteresis uses two thresholds and if the magnitude is below the first threshold, it is set to zero. If the magnitude is above the high threshold, it is made an edge. And if the magnitude is between the 2 thresholds, then it is set to zero unless there is a path from this pixel to a pixel with a gradient above T2.

-1	0	+1
-2	0	+2
-1	0	+1

G_x

+1	+2	+1
0	0	0
-1	-2	-1

G_y

Figure 3.10 Masks for the Canny gradient edge detector [7]

The magnitude, or edge strength, of the gradient is then approximated using the formula:

$$|G| = |G_x| + |G_y| \quad \ldots\ldots (24)$$

The edge direction is:

$$\theta = \tan^{-1}\left(\frac{G_y}{G_x}\right) \quad \ldots\ldots (25)$$

3.3.6. Morphological Based Operation

The fundamental operations associated with an object are the standard set operations union, intersection, complement and translation [6] and [7]:

Translation - Given a vector x and a set A, the translation, A + x, is defined as:

$$A + x = \{\alpha + x | \alpha \in A\} \dots\dots\dots\dots\dots\dots\dots\dots\dots\dots\dots\dots\dots\dots\dots\dots\dots\dots . . (26)$$

If a digital image is composed of pixels at integer coordinate positions, this implies restrictions on the allowable translation vectors x.

The basic Minkowski set operations [6] and [7] addition and subtraction can now be defined. First it is to note that the individual elements that comprise B are not only pixels but also vectors as they have a clear coordinate position with respect to [0, 0]. Given two sets A and B:

Minkowski addition -

$$A \oplus B = \bigcup_{\beta \in B} (A + \beta) \dots\dots\dots\dots\dots\dots\dots\dots\dots\dots\dots\dots\dots\dots\dots\dots\dots\dots (27)$$

Minkowski subtraction –

$$A \ominus B = \bigcap_{\beta \in -B} (A + \beta) \dots\dots\dots\dots\dots\dots\dots\dots\dots\dots\dots\dots . \dots\dots\dots\dots (28)$$

From these two Minkowski operations can be defined the fundamental mathematical morphology operations dilation and erosion:

Dilation –

$$D(A, B) = A \oplus B \dots\dots\dots\dots\dots\dots\dots\dots\dots\dots\dots\dots\dots\dots\dots\dots\dots\dots\dots\dots . (29)$$

Erosion –

$$E(A, B) = A \ominus (-B) \dots\dots\dots\dots\dots\dots\dots\dots\dots\dots\dots\dots . \dots\dots\dots\dots\dots\dots\dots\dots (30)$$

CHAPTER 4

Simulation Environment

4.1. Materials

T1 weighted, T2 weighted and proton density MR images of brain has been used. The main purposes of these images are for segmentation of CSF, GM and WM on brain image.

4.2. Software Tools

MATLAB 7.0 and Visual Basic 6.0 have been used as programming tool.

4.3. Hardware

The MATLAB 7.0 and visual Basic 6.0 code for image segmentation has been developed on Laptop with specifications:- Intel Dual Core 1.46 GHz CPU, 1 GB RAM and Windows Vista operating system.

CHAPTER 5

Experimental Study

In this section implementation of this thesis is explained. The MR image of brain is taken for implementation. There are two algorithms: EM and k-NN implemented for the segmentation of MR image of brain. The comparison between those two algorithms is also discussed in this section.

5.1. Implementation of Expectation Algorithm

First of all histogram is plotted as shown in figure 5.2. The mean and variance are the variables for expectation maximization (EM) algorithm. The mean and variance are expected. The Gaussian distribution with initial expected value is as shown in figure 5.1. The expected values of mean and variance are fed to EM algorithm till the convergence. The value of mean and variance obtained from EM algorithm is passed to the Gaussian distribution. The new Gaussian distribution is as shown in figure 5.5.

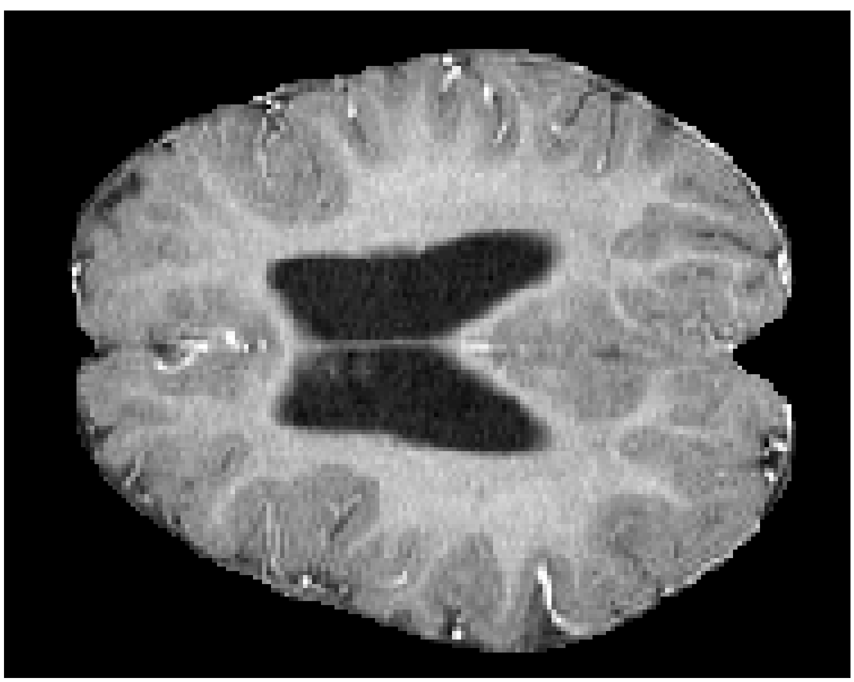

Figure 5.1 Test image

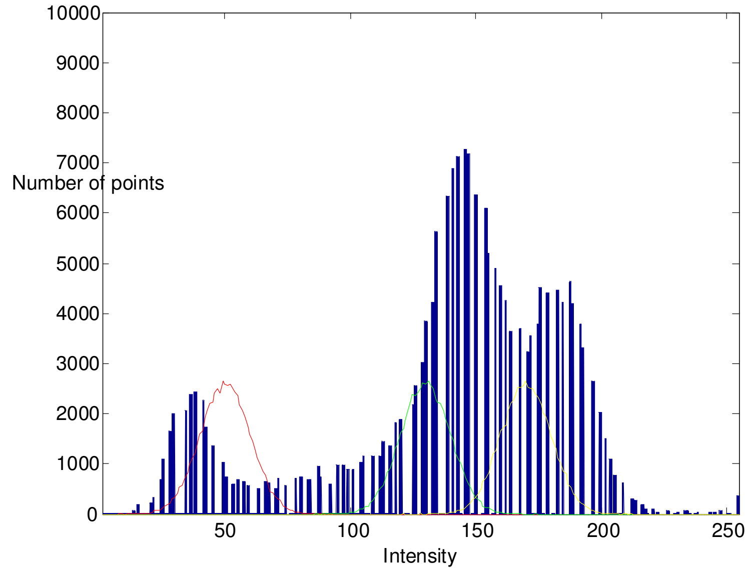

Figure 5.2 Histogram of test image

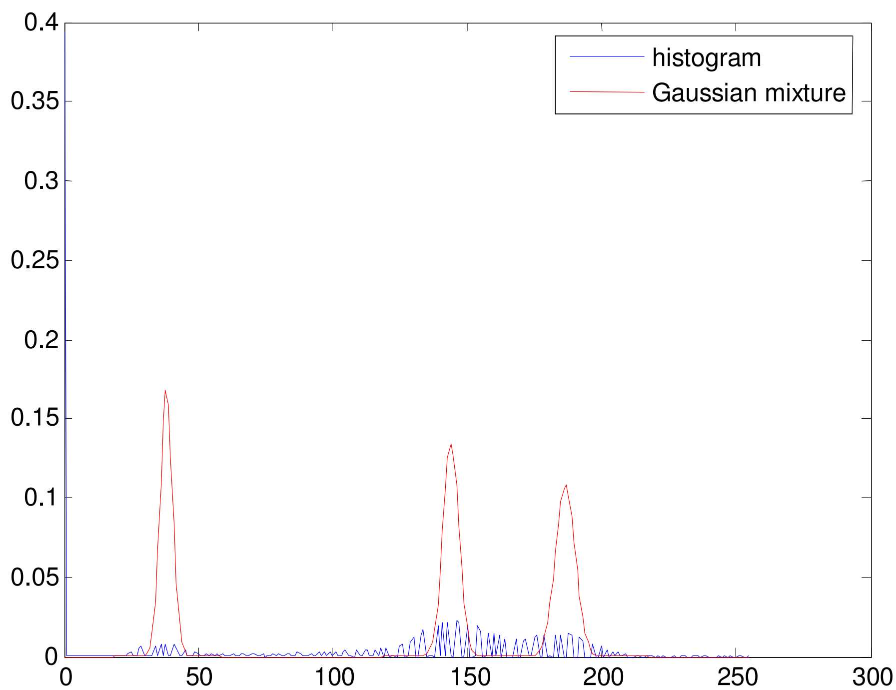

Figure 5.3 Histogram and Gaussian Mixture

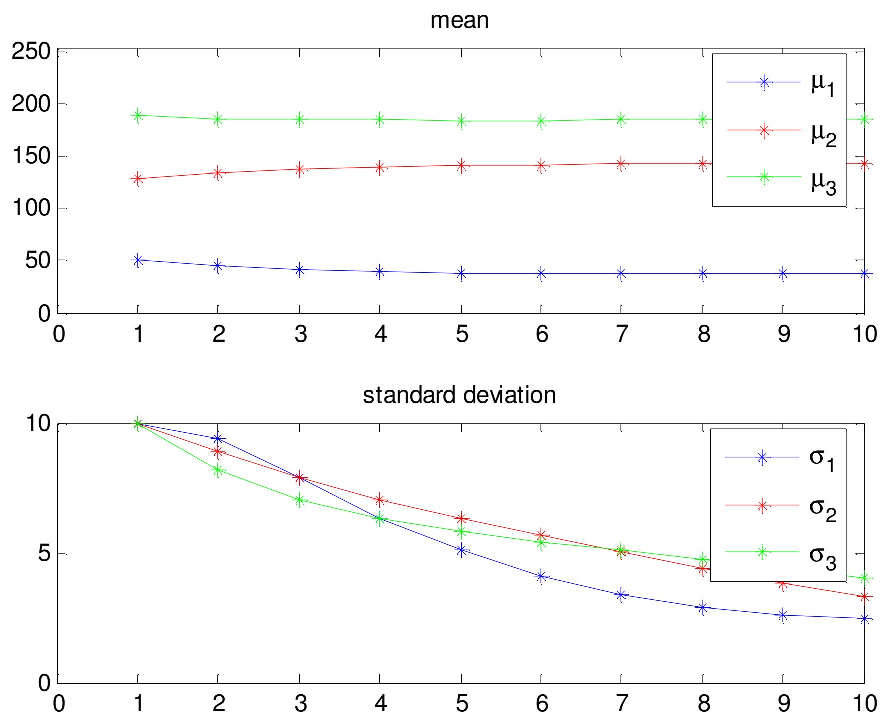

Figure 5.4 Mean and Standard Deviation

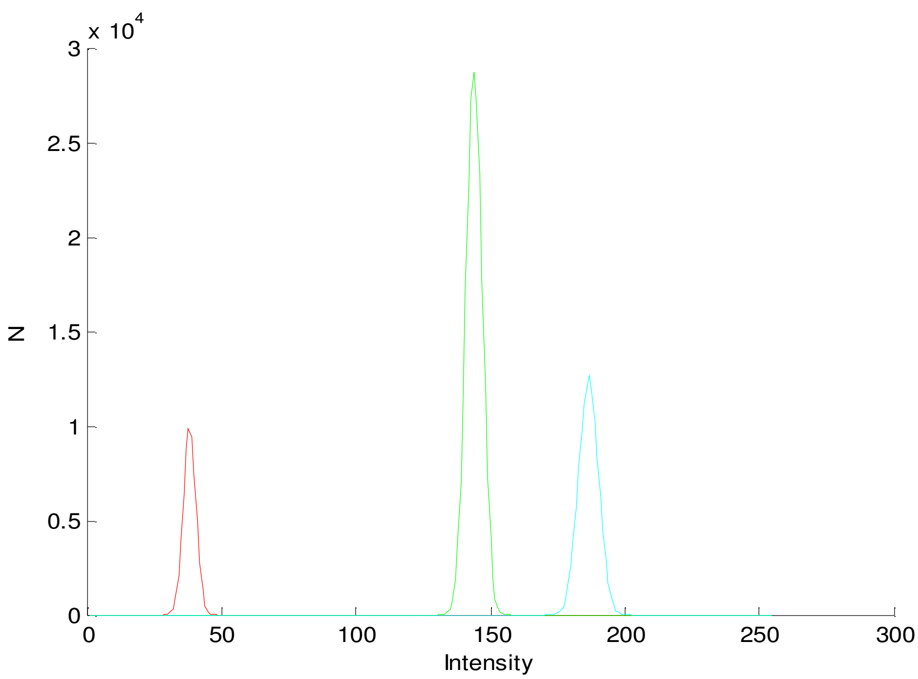

Figure 5.5 Individual Gaussian Curves

The MR image of brain has been segmented into gray matter (GM), white matter (WM) and cerebral spinal fluid (CSF).

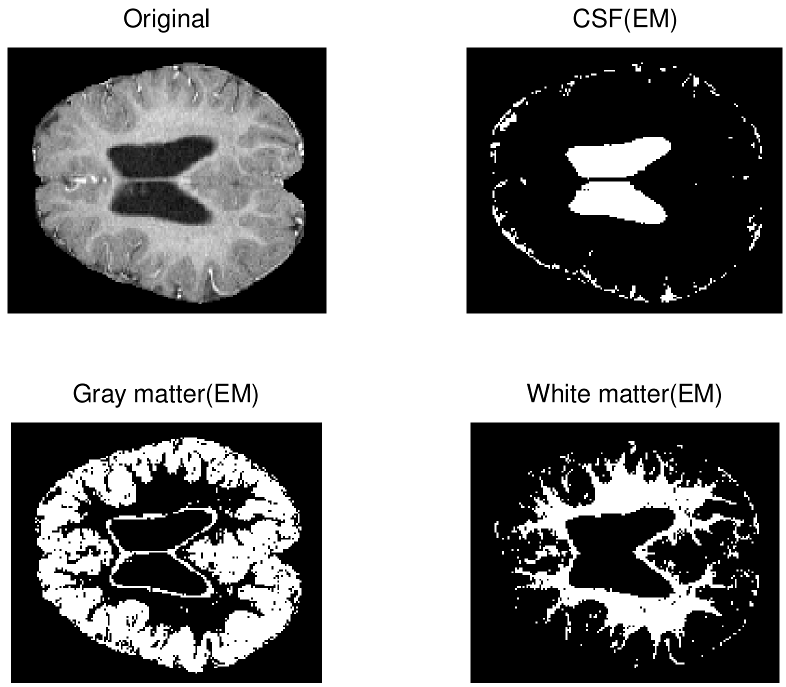

Figure 5.6 Brain image segmentation using EM algorithm

With the help of morphological operation i.e. dilation boundary between different space has been extracted.

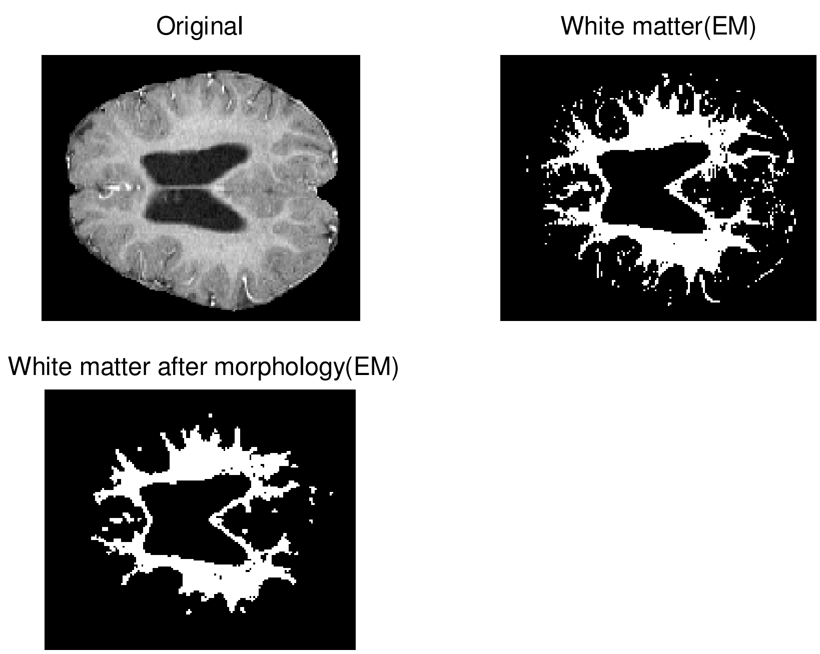

Figure5.7 Extraction of white matter using morphological operation

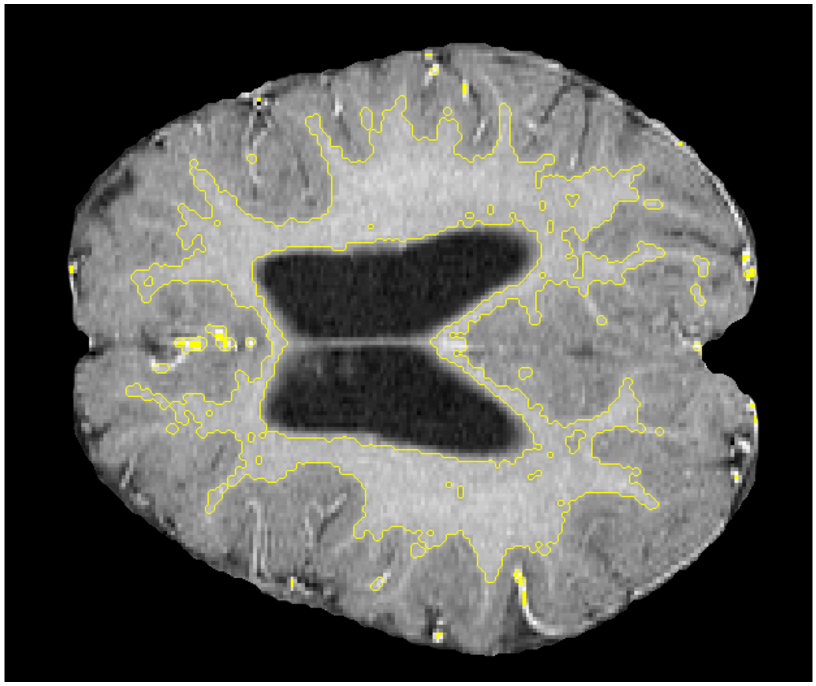

Figure 5.8 Boundary for white matter

5.2. Implementation of k-NN Algorithm

First of all, as explanation in chapter 4, k numbers of pixels are taken for each CSF, GM and WM regions. These pixels are training samples for k-NN algorithm. Each pixel of the MR- image is fed to k-NN algorithm. Euclidian distance between the query instance and training samples is calculated using equation no. (15). Then determine the nearest neighbor based on k-th minimum distance. The threshold points for each region are calculated. The plot of threshold for different regions is as shown in figure 5.9

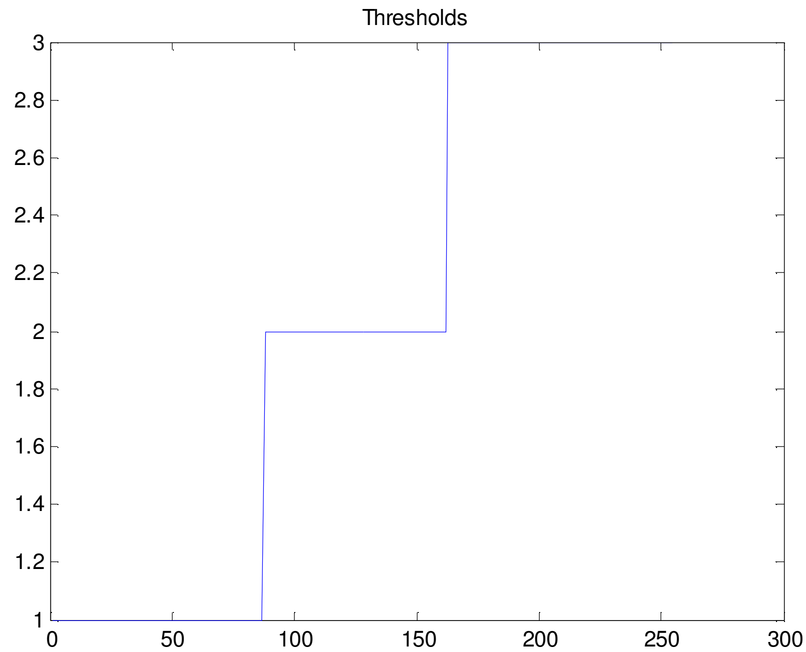

Figure 5.9 Threshold

The MR image of brain has been segmented into gray matter (GM), white matter (WM) and cerebral spinal fluid (CSF).

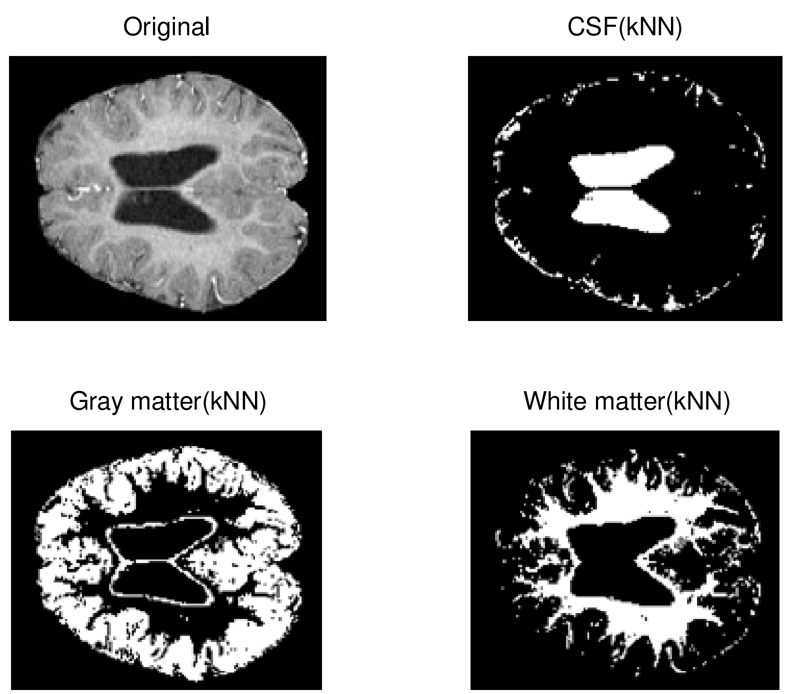

Figure 5.10 Segmentation using k-NN Algorithm

With the help of morphological operation i.e. dilation boundary between different spaces has been extracted.

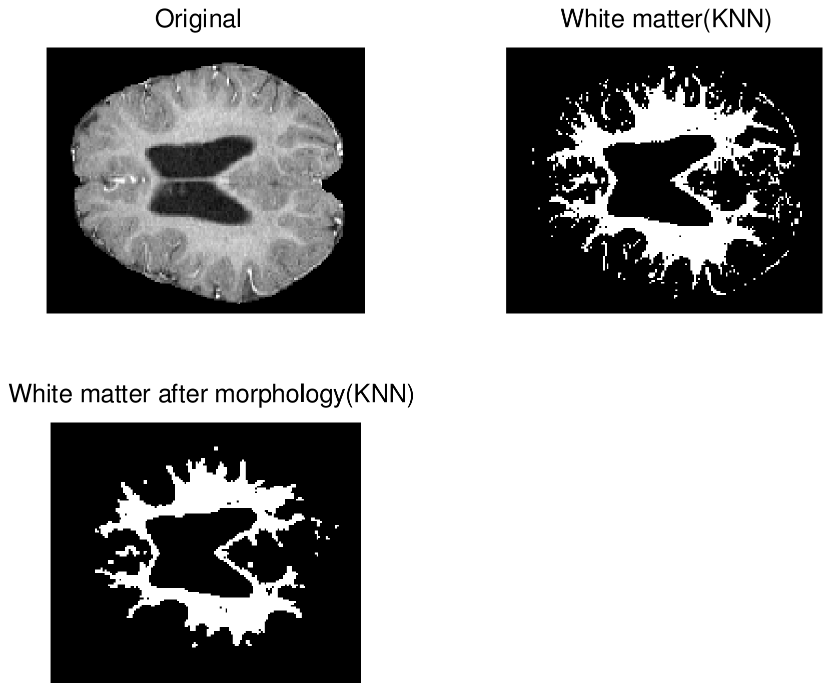

Figure 5.11 Extraction of white matter with Morphological operation

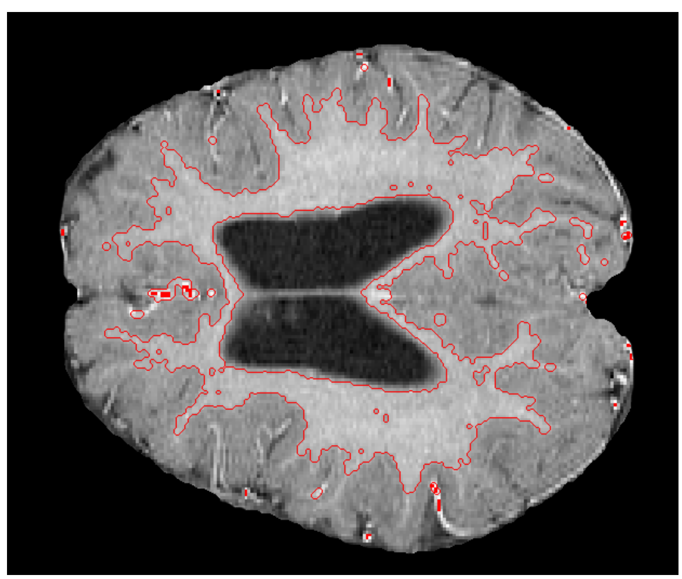

Figure 5.12 Boundary for white matter

5.3. Comparison between EM and k-NN Algorithms

The comparative results between the EM and k-NN algorithms are presented in figure 5.13, 5.14 and 5.15 and table 5.1 and 5.2.

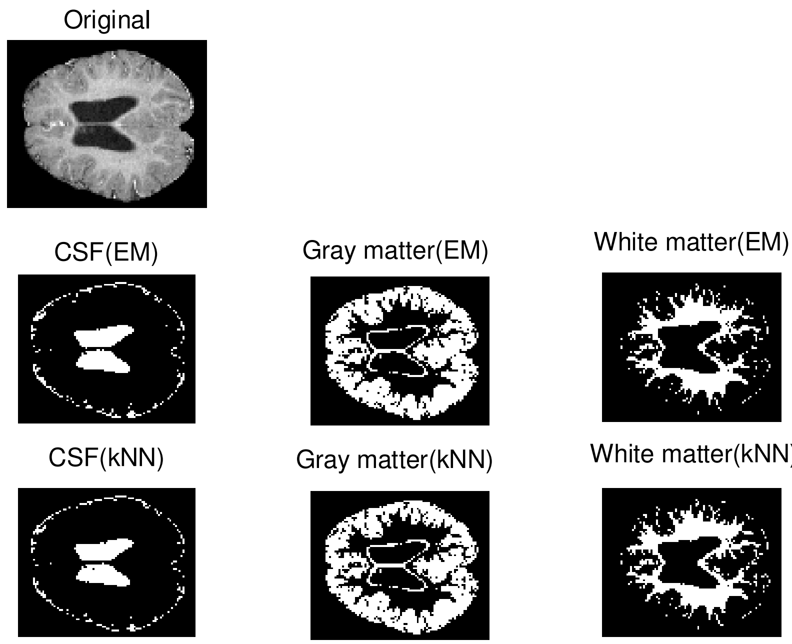

Figure 5.13 Comparison between segmentation using EM and k-NN algorithm for image 1

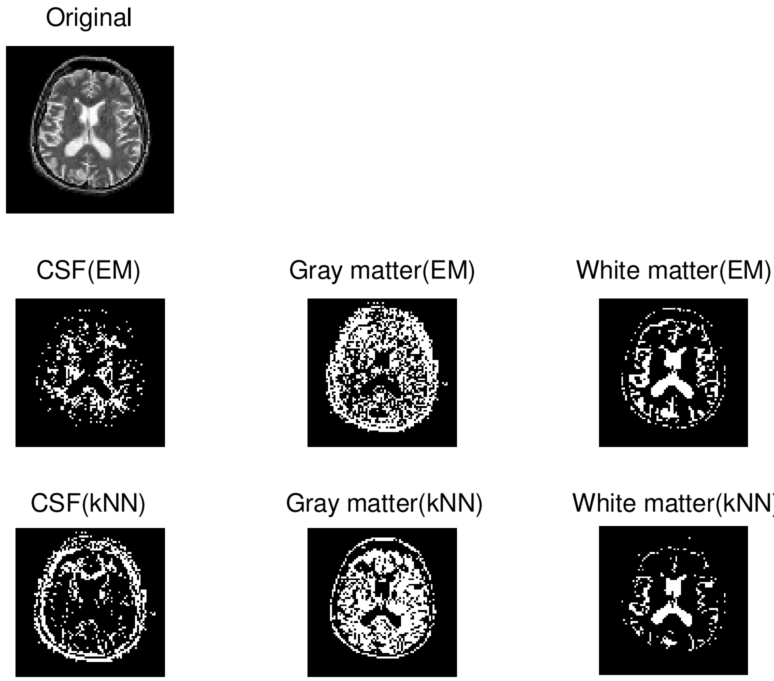

Figure 5.14 Comparison between segmentation using EM and k-NN algorithm for image 2

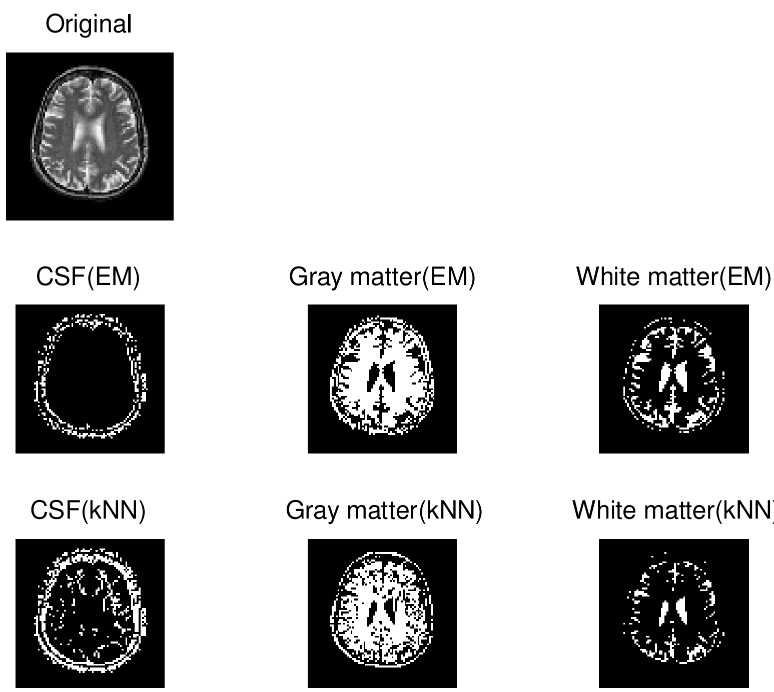

Figure 5.15 Comparison between segmentation using EM and k-NN algorithm for image 3

Image	Algorithm	% of CSF	% of GM	% of WM
1	EM	16.3465	54.8433	28.8102
	k-NN	15.5832	53.2800	31.1368
2	EM	18.7317	54.6759	26.5924
	k-NN	33.4368	50.4578	16.1054
3	EM	14.3366	62.3677	23.2957
	k-NN	29.8292	56.4828	13.6880

Table 5.1 Comparison between EM and k-NN algorithms (vollume)

Image	1	2	3
EM	0.421000 seconds.	0.249000 seconds.	0.234000 seconds.
k-NN	0.468000 seconds.	0.375000 seconds.	0.297000 seconds.

Table 5.2 Comparison between EM and k-NN algorithms (execution time)

CHAPTER 6

Conclusion and Future Enhancement

5.1. Conclusion

In this thesis, the Expectation Maximization (EM) and k Nearest Neighbor (k-NN) algorithms have been implemented for segmentation of MR images of brain. The computation time for EM algorithm is smaller than that of k-NN algorithm. The brain image is segmented into cerebral spinal fluid (CSF), gray matter (GM) and white matter (WM). The segmentation of MR images of brain can be used for medical diagnosis process.

Finally, this thesis work is for the segmentation of MR images of brain, but can be implemented for segmentation of other kind of images.

5.2. Future Enhancement

The segmentation of brain image into GM, WM and CSF is completed using EM algorithm and kNN algorithm. Detection of tumor tissue and localization of it is the future enhancement of this thesis.

References

1. S. K. Pal and P. Mitra, “Multispectral Image Segmentation Using the Rough-Set-Initialized EM Algorithm” ieee Transactions on Geoscience and Remote Sensing, Vol. 40, No. 11, pp. 2495- 2501, November 2002.

2. Elizabeth Berry, “A Practical Approach to Medical Image Processing” Taylor & Francis Group, 2008

3. S. Tatiraju and A. Metha, “Image Segmentation Using K-Means Clustering EM and Normalized Cuts”.

4. S Saha and S. Bandyopadhyay “MRI Brain Image Segmentation by Fuzzy Symmetry Based Genetic Clustering Technique” ieee CEC 2007.

5. R. Cardenes, M. Batch, Y. Chi, I. Marras, R. de Luis, M. Anderson, P. Chasman and M. Butelle, “Multimodal Evalution for Medical Image Segmentation”

6. Anil K. Jain, “Fundamental of Digital Image Processing” Prentice-Hall Inc. 1989

7. R. C. Gonzalez, R. E. Woods, “Digital Image Processing”, Pearson Education, Inc. Second Edition, 2002

8. Keith A, Johnson, M.D. J. Alex Becker, “The Whole Brain Atlas” http://www.med.harvard.edu/AANLIB/home.html

9. M. Murgasova, L. Dyet, J. Hajnal, “Robust segmentation of brain MRI using combination of registration and EM- based methods”

10. M. F. Tolba, M. G. Mostafa, T. F. Gharib, M. A-Megeed, “ MR- Brain Image Segmentation using Gaussian Multiresolution Analysis and The EM Algorithm”

11. S. Chen, L. Cao, J. Liu, X. Tang, “Iterative MAP and ML Estimations for Image Segmentation” IEEE 2007

12. D. Sen, S. K. Pal, “Histogram Thresholding using Fuzzy and Rough Measures of Association Error” IEEE Transactions on Image Processing, Vol. 18, No. 4, April 2009

13. R. Cardenes, M. R. Sanchez and J. Ruiz-Alzola, “Computational Geometry Computation and kNN Segmentation in ITK”, August 2006.

14. Y. Li and Z. Chi, “MR Brain Segmentation Based on Self-Organizing Network” IJIT, Vol. 11 No. 8, 2005

15. B. Koyuncu and A. Pasha, “Contour Profiling of Brain tumor Areas by Using Image Correlation and Peak Detection Techniques’ IJCNS Vol. 6 No. 11. November 2006.

Appendix

Result From Visual Basics

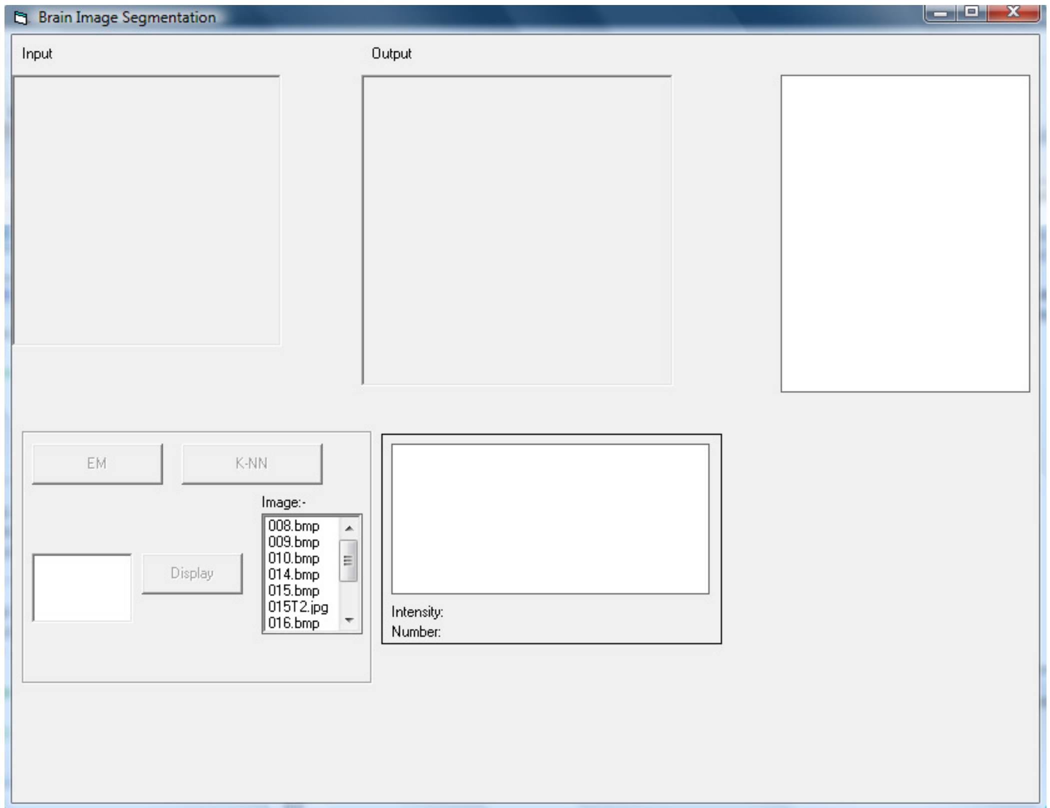

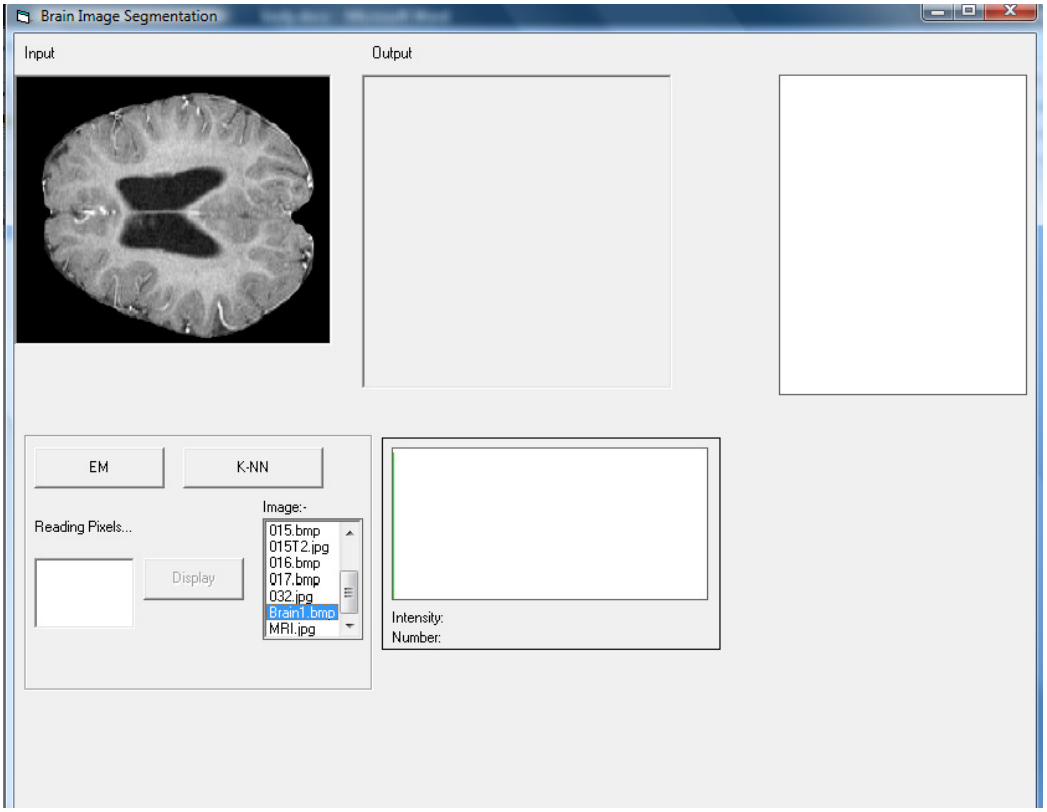
Brain Image Segmentation
Input
Output
EM
K-NN
Image:-
Reading Pixels...
Display
015.bmp
015T2.jpg
016.bmp
017.bmp
032.jpg
Brain1.bmp
MRI.jpg
Intensity:
Number:

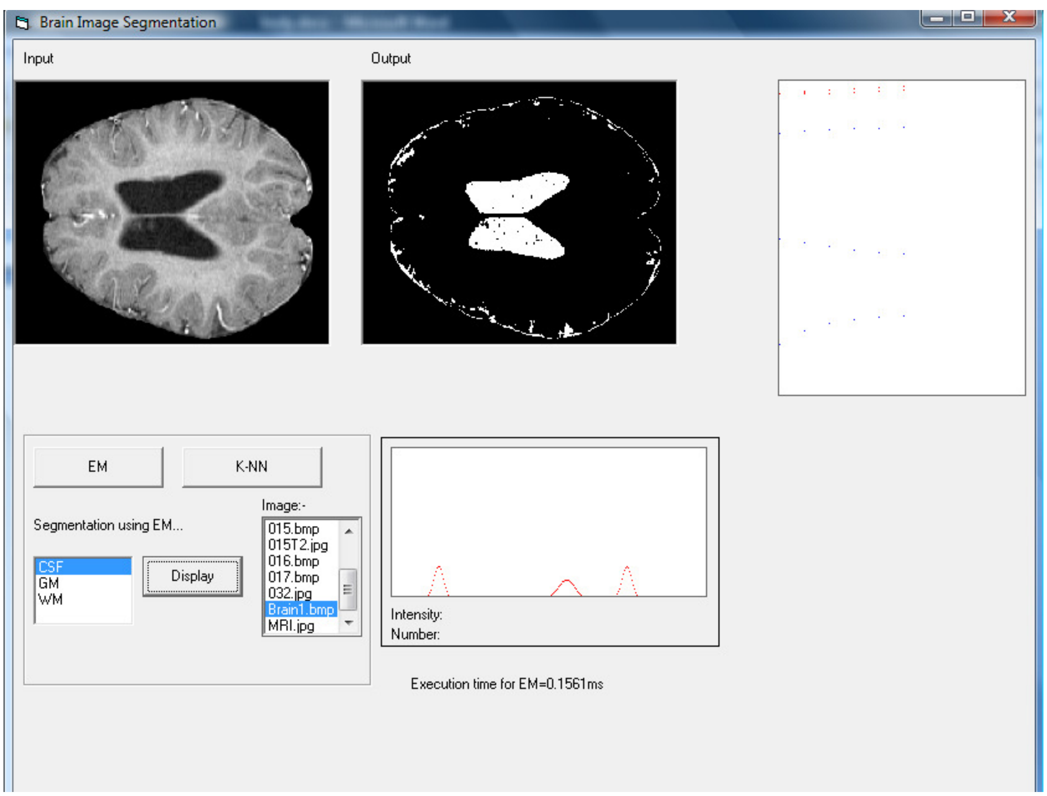
Brain Image Segmentation
Input
Output
EM
K-NN
Image:-
Segmentation using EM...
CSF
GM
WM
Display
015.bmp
015T2.jpg
016.bmp
017.bmp
032.jpg
Brain1.bmp
MRI.jpg
Intensity:
Number:
Execution time for EM=0.1561ms

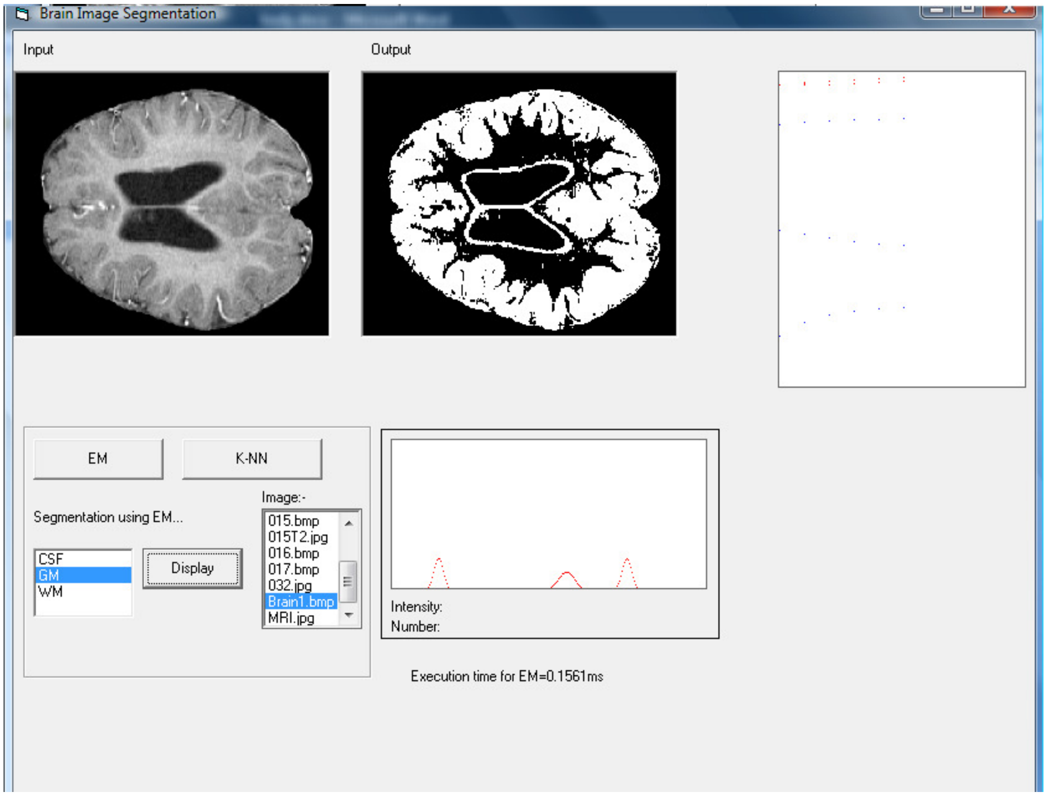
Brain Image Segmentation
Input
Output
EM
K-NN
Image:-
Segmentation using EM...
015.bmp
015T2.jpg
016.bmp
017.bmp
032.jpg
Brain1.bmp
MRI.jpg
CSF
GM
WM
Display
Intensity:
Number:
Execution time for EM=0.1561ms

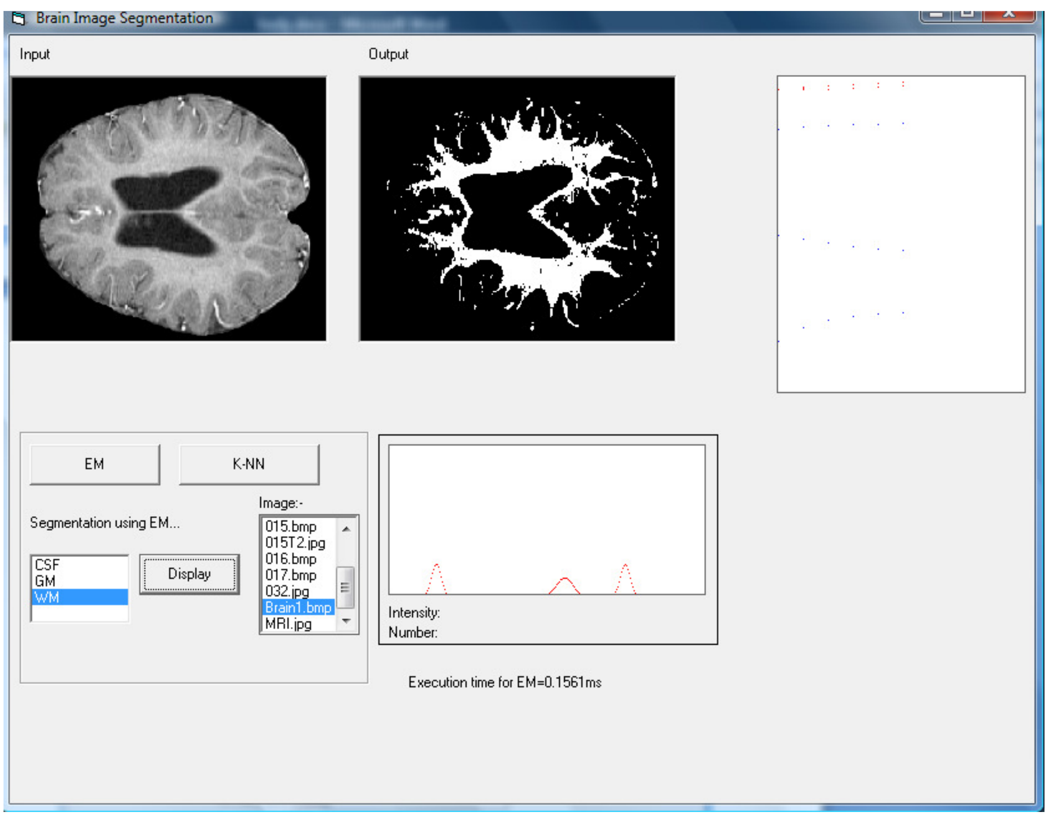
Brain Image Segmentation
Input
Output
EM
K-NN
Image:-
Segmentation using EM...
015.bmp
015T2.jpg
016.bmp
017.bmp
032.jpg
Brain1.bmp
MRI.jpg
CSF
GM
WM
Display
Intensity:
Number:
Execution time for EM=0.1561ms

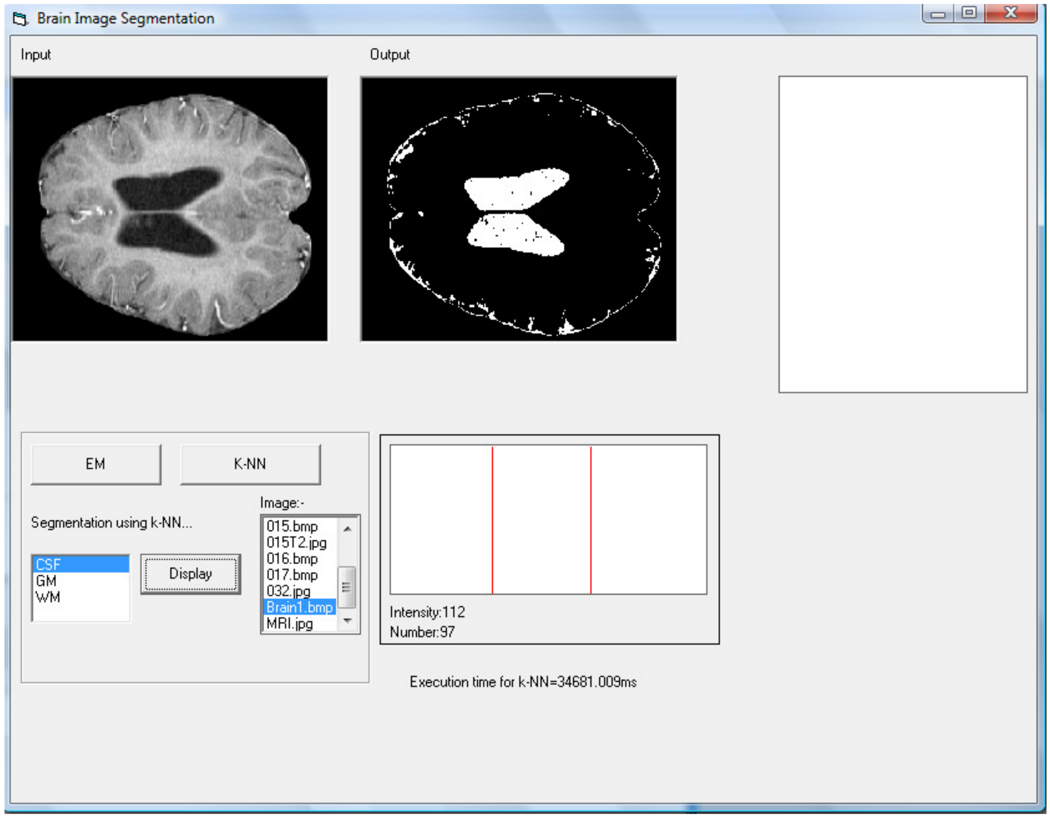

Brain Image Segmentation
Input
Output
EM
K-NN
Image:-
Segmentation using k-NN...
CSF
GM
WM
Display
015.bmp
015T2.jpg
016.bmp
017.bmp
032.jpg
Brain1.bmp
MRI.jpg
Intensity:112
Number:97
Execution time for k-NN=34681.009ms

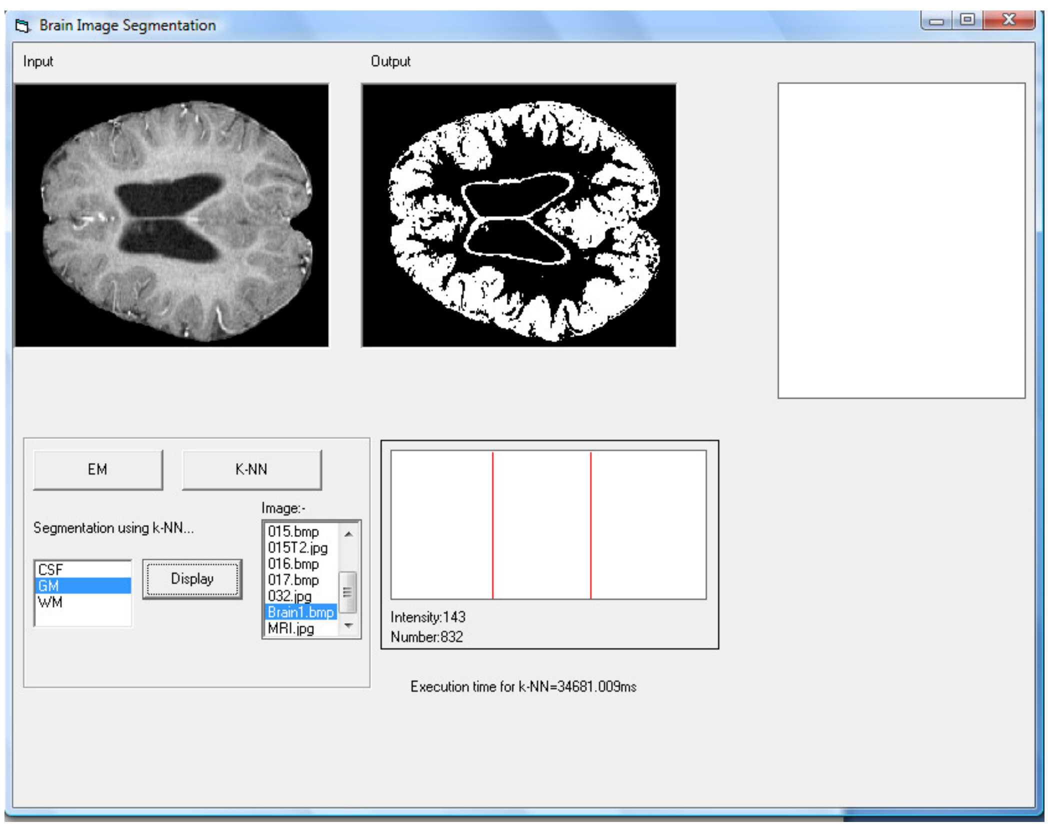

Brain Image Segmentation
Input
Output
EM
K-NN
Image:-
Segmentation using k-NN...
CSF
GM
WM
Display
015.bmp
015T2.jpg
016.bmp
017.bmp
032.jpg
Brain1.bmp
MRI.jpg
Intensity:143
Number:832
Execution time for k-NN=34681.009ms

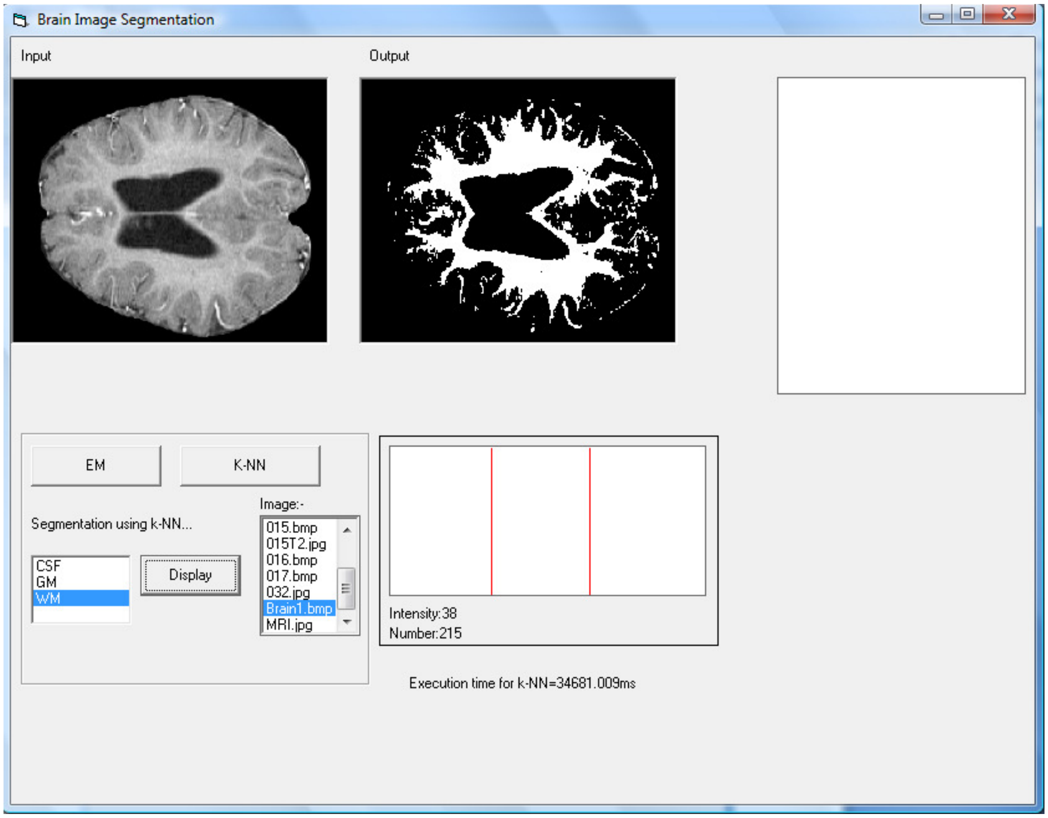
Brain Image Segmentation
Input
Output
EM
K-NN
Image:-
Segmentation using k-NN...
CSF
GM
WM
Display
015.bmp
015T2.jpg
016.bmp
017.bmp
032.jpg
Brain1.bmp
MRI.jpg
Intensity:38
Number:215
Execution time for k-NN=34681.009ms